

Measurement of the W Boson Mass with 1 fb^{-1} of D0 Run II Data

Mikolaj Cwiok^{*†}

University of Warsaw, Faculty of Physics, Poland

E-mail: Mikolaj.Cwiok@fuw.edu.pl

We present the most precise single measurement of the W boson mass using data collected with the D0 experiment. An integrated luminosity of 1 fb^{-1} yields 499,830 $W \rightarrow e\nu$ candidates. With this sample we measure $M_W = 80.401 \pm 0.043 \text{ GeV}$.

*The 2009 Europhysics Conference on High Energy Physics,
July 16 - 22 2009
Krakow, Poland*

^{*}Speaker.

[†]For the D0 Collaboration

Precise knowledge of the W boson mass (M_W) is an important contribution to our understanding of the electroweak fundamental force. Experimental measurements of the M_W and the top quark mass allow to tighten constraints on the mass of the Higgs boson from internal consistency of the Standard Model. The current world-average value is $M_W = 80.399 \pm 0.025$ GeV [1] from a combination of results of LEP [2] and Tevatron [3, 4] experiments.

In these Proceedings we present a measurement of M_W using data from $p\bar{p}$ collisions at $\sqrt{s} = 1.96$ TeV collected between 2002 and 2006 with the D0 detector [5] and corresponding to a total integrated luminosity of 1 fb^{-1} . Because the D0 calorimeter is well-suited for a precise measurement of electron energies we use $W \rightarrow e\nu$ decay mode. The M_W is measured using three kinematic variables defined in the plane perpendicular to the beam direction: the transverse mass $m_T = \sqrt{2p_T^e p_T^\nu (1 - \cos \Delta\phi_{e\nu})}$ (where $\Delta\phi_{e\nu}$ is the opening angle between the electron and neutrino momenta in the plane transverse to the beam), the electron transverse momentum p_T^e and the neutrino transverse momentum p_T^ν . The magnitude and direction of \vec{p}_T^ν are inferred from the event missing transverse energy \vec{E}_T . The data spectra of m_T , p_T^e and \vec{E}_T are compared with spectra (templates) from Monte Carlo simulation with varying input M_W values.

The D0 detector [5] contains tracking, calorimeter and muon systems. The tracking system consists of the inner Silicon Microstrip Tracker and the outer Central Fiber Tracker covering pseudorapidity $|\eta| \lesssim 3$ and $|\eta| \lesssim 2$ respectively. The tracking detectors are surrounded by a 2 T solenoid magnet. Three uranium, liquid-argon calorimeters measure particle energies. The Central Calorimeter (CC) covers $|\eta| < 1.1$ and two End Calorimeters (EC) extend coverage up to $|\eta| \approx 4.2$. The CC is segmented in depth into eight layers. The first four are used as an electromagnetic calorimeter (EM). A three level trigger system selects events for recording with a rate of 100 Hz.

W and Z boson events are selected using a trigger requiring at least one EM cluster in the CC with transverse energy above $20 \div 25$ GeV depending on run conditions. Candidate W boson events are required to have one EM cluster reconstructed in the CC, with $p_T^e > 25$ GeV and $|\eta| < 1.05$. The EM cluster must pass electron shower shape and energy isolation criteria in the calorimeter, be within the central 80% of the electromagnetic section of each CC module, and have one track matching in (η, ϕ) space, where the track has at least one hit in the silicon tracker and $p_T > 10$ GeV. The event must satisfy: $E_T > 25$ GeV, $u_T < 15$ GeV and $50 < m_T < 200$ GeV, where E_T is the magnitude of the vector sum of the transverse energy of calorimeter cells above read out threshold, and u_T is the magnitude of the vector sum of the transverse component of the energies measured in calorimeter cells excluding those associated with the reconstructed electron. This selection yields 499,830 candidate $W \rightarrow e\nu$ events. We use $Z \rightarrow ee$ events for calibration. Candidate Z boson events are required to have: two EM clusters satisfying same requirements as $W \rightarrow e\nu$ events, both electrons having $p_T^e > 25$ GeV, $u_T < 15$ GeV and the invariant mass of the dielectron pair $70 \leq m_{ee} \leq 110$ GeV. Events with both electrons in the CC are used to determine the EM calibration. This selection yields 18,725 candidate $Z \rightarrow ee$ events.

The backgrounds in the W boson sample are: $Z \rightarrow ee$ events in which one electron escapes detection, multijet events in which a jet is misidentified as an electron with \vec{E}_T arising from misreconstruction, and $W \rightarrow \tau\nu \rightarrow e\nu\nu\nu$ events. The background from Z boson events arises from electrons which traverse the gap between the CC and EC. The backgrounds expressed as a fraction of the final W boson sample are: $(0.90 \pm 0.01)\%$ from $Z \rightarrow ee$, $(1.49 \pm 0.03)\%$ from multijet and

Variable	Fit Range (GeV)	M_W (GeV)	χ^2/dof
m_T	$65 < m_T < 90$	80.401 ± 0.023	48/49
p_T^e	$32 < p_T^e < 48$	80.400 ± 0.027	39/31
\cancel{E}_T	$32 < \cancel{E}_T < 48$	80.402 ± 0.023	32/31

Table 1: Results from the fits to data. Only the statistical uncertainty is shown.

$(1.60 \pm 0.02)\%$ from $W \rightarrow \tau\nu \rightarrow e\nu\nu\nu$.

W and Z boson production and decay kinematics are simulated using the RESBOS [6] next-to-leading order generator which includes non-perturbative effects at low boson p_T . The radiation of one or two photons is performed using the PHOTOS [7] program. A fast parametric Monte Carlo simulation (FASTMC) applies detector efficiencies, energy response and resolution effects for the electron and hadronic energy to the RESBOS+PHOTOS events. The FASTMC parameters are determined using a combination of detailed simulation and control data samples.

The Z boson mass measured precisely at LEP [8] is used to calibrate our EM calorimeter response assuming a form $E^{\text{meas}} = \alpha E^{\text{true}} + \beta$. Thus, the M_W measurement presented here is effectively a measurement of the ratio of W and Z boson masses. The hadronic response (resolution) is tuned by using the mean (width) of the η_{imb} distribution in $Z \rightarrow ee$ events in different bins of dielectron transverse momentum p_T^{ee} , where η_{imb} is a projection of $(\vec{p}_T^{ee} + \vec{u}_T)$ vector on the axis bisecting the dielectron opening angle [9].

The FASTMC template distributions for m_T , p_T^e and \cancel{E}_T are generated at different M_W values with intervals of 10 MeV and backgrounds are added to the simulated distributions. A binned likelihood between the data and each template is then computed. The resulting log likelihoods as a function of mass are fit to a parabola to determine measured M_W value, separately for each of three distributions. Before analyzing the collider data a test of the analysis method is performed using events produced by the detailed GEANT [10] Monte Carlo simulation treated as collider data, including the FASTMC tuning with the simulated $Z \rightarrow ee$ events. The M_W fit results for all three kinematic distributions agree with the input M_W value within 20 MeV of total uncertainty.

The FASTMC tuning for the collider data and internal consistency checks are done without knowledge of the final result. The M_W values returned from fits are blinded by means of adding an unknown constant offset, the same for m_T , p_T^e and \cancel{E}_T observables. The results are unblinded once the important data and FASTMC comparison plots have acceptable χ distributions. Table 1 shows the M_W fit results after unblinding. Comparisons between the data and FASTMC templates with background for the best M_W fit are shown in Fig. 1.

The systematic uncertainties in the M_W measurement due to experimental sources and the production mechanism are summarized in Table 2. The electron energy calibration and resolution, and hadronic recoil model uncertainties are determined by varying the FASTMC parameters by one statistical standard deviation including correlation coefficients. The shower modelling uncertainties are determined by varying the amount of material representing the detector in the detailed GEANT simulation. A possible systematic bias for the energy loss differences arising from different energy or pseudorapidity distributions for the electrons from W and Z boson decays is negligible. The quoted systematic uncertainty is due to the finite statistics of the detailed simulation. The

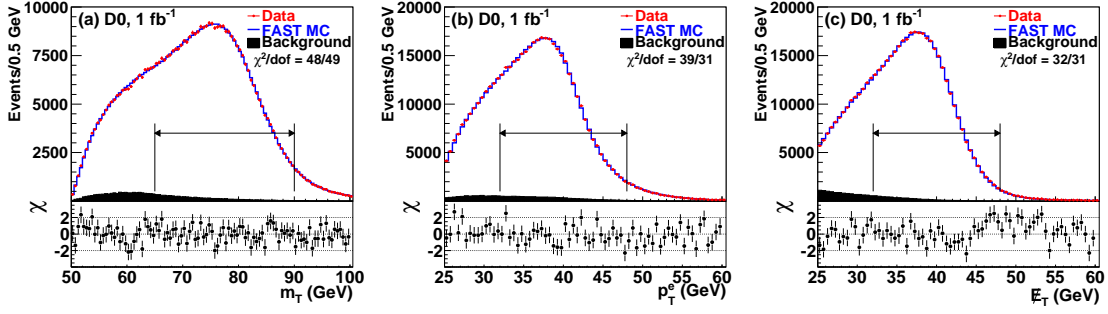


Figure 1: The (a) m_T , (b) p_T^e and (c) E_T distributions for data and FASTMC simulation with backgrounds. The χ values are shown below each distribution. The double-ended horizontal arrows indicate fit ranges.

Source	ΔM_W (MeV)		
	m_T	p_T^e	E_T
Electron energy calibration	34	34	34
Electron resolution model	2	2	3
Electron shower modelling	4	6	7
Electron energy loss model	4	4	4
Hadronic recoil model	6	12	20
Electron efficiencies	5	6	5
Backgrounds	2	5	4
Experimental Subtotal	35	37	41
PDF	10	11	11
QED	7	7	9
Boson p_T	2	5	2
Production Subtotal	12	14	14
Total	37	40	43

Table 2: Systematic uncertainties of the M_W measurement.

uncertainty due to parton distribution function (PDF) is computed using CTEQ prescription [11]. The comparison of WGRAD [12] and ZGRAD [13] generators with PHOTOS are used to assess the QED uncertainty. The boson p_T uncertainty is obtained by varying g_2 parameter of the RESBOS generator by its quoted uncertainty [14]. In order to test stability of the fits the data are also subdivided into statistically independent categories based on: instantaneous luminosity, time, the total hadronic transverse energy in the event, the vector sum of the hadronic energy and electron pseudorapidity range. The fit ranges are also varied. For each of these tests the results are stable within the measurement uncertainty.

The results from three observables are combined using the BLUE method [15] including statistical and systematic correlation coefficients determined from ensembles of simulated events. The correlation coefficients are 0.83, 0.82 and 0.68 for (m_T, p_T^e) , (m_T, E_T) and (p_T^e, E_T) respectively.

The final, combined result is

$$\begin{aligned} M_W &= 80.401 \pm 0.021 \text{ (stat)} \pm 0.038 \text{ (syst)} \text{ GeV} \\ &= 80.401 \pm 0.043 \text{ GeV.} \end{aligned}$$

It agrees well with the world average [1] and at present is more precise than any other single measurement. Since the dominant uncertainties arise from the limited statistics of the $W \rightarrow e\nu$ and $Z \rightarrow ee$ samples this measurement is expected to improve when more data are analyzed.

References

- [1] The LEP Electroweak Working Group, CERN-PH-EP/2008-20, arXiv:0811.4682 [hep-ex] (2008), and The Tevatron Electroweak Working Group, FERMILAB-TM-2415 (2008). More information is available at: <http://tevewwg.fnal.gov>.
- [2] S. Schael *et al.* (ALEPH Collaboration), *Eur. Phys. J. C* **47**, 309 (2006); J. Abdallah *et al.* (DELPHI Collaboration), *Eur. Phys. J. C* **55**, 1 (2008); P. Achard *et al.* (L3 Collaboration), *Eur. Phys. J. C* **45**, 569 (2006); G. Abbiendi *et al.* (OPAL Collaboration), *Eur. Phys. J. C* **45**, 307 (2006).
- [3] B. Abbott *et al.* (D0 Collaboration), *Phys. Rev. D* **58**, 092003 (1998); B. Abbott *et al.* (D0 Collaboration), *Phys. Rev. D* **62**, 092006 (2000); V. M. Abazov *et al.* (D0 Collaboration), *Phys. Rev. D* **66**, 012001 (2002).
- [4] T. Affolder *et al.* (CDF Collaboration), *Phys. Rev. D* **64**, 052001 (2001); T. Aaltonen *et al.* (CDF Collaboration), *Phys. Rev. Lett.* **99**, 151801 (2007); T. Aaltonen *et al.* (CDF Collaboration), *Phys. Rev. D* **77**, 112001 (2008).
- [5] V. M. Abazov *et al.* (D0 Collaboration), *Nucl. Instrum. Methods in Phys. Res. A* **565**, 463 (2006).
- [6] C. Balazs and C.P. Yuan, *Phys. Rev. D* **56**, 5558 (1997).
- [7] E. Barberio and Z. Was, *Comput. Phys. Commun.* **79**, 291 (1994).
- [8] C. Amsler *et al.*, *Phys. Lett. B* **667**, 1 (2008) and references therein.
- [9] J. Alitti *et al.* (UA2 Collaboration), *Phys. Lett. B* **276**, 354 (1992).
- [10] R. Brun and F. Carminati, CERN Program Library Long Writeup W5013 (1993).
- [11] H.L. Lai *et al.*, *Phys. Rev. D* **55**, 1280 (1997); D. Stump *et al.*, *JHEP* **0310**, 046 (2003).
- [12] U. Baur *et al.*, *Phys. Rev. D* **59**, 013002 (1998).
- [13] U. Baur *et al.*, *Phys. Rev. D* **57**, 199 (1998); U. Baur *et al.*, *Phys. Rev. D* **65**, 033007 (2002).
- [14] F. Landry, R. Brock, P. Nadosky, and C.P. Yuan, *Phys. Rev. D* **67**, 073016 (2003). The BLNY parameterization, eqn. 12, is used.
- [15] L. Lyons, D. Gibout, and P. Clifford, *Nucl. Instrum. Methods in Phys. Res. A* **270**, 110 (1988); A. Valassi, *Nucl. Instrum. Methods in Phys. Res. A* **500**, 391 (2003).